European Journal of Pharmaceutics and Biopharmaceutics 137 (2019) 185–195

Contents lists available at ScienceDirect

European Journal of Pharmaceutics and Biopharmaceutics

journal homepage: www.elsevier.com/locate/ejpb

Research paper

Liposome-targeted recombinant human acid sphingomyelinase: Production, formulation, and *in vitro* evaluation

Mohammed H. Aldosari[a,b], Robert P. de Vries[c], Lucia R. Rodriguez[a], Nienke A. Hesen[a], Nataliia Beztsinna[a], André B.P. van Kuilenburg[d], Carla E.M. Hollak[e], Huub Schellekens[a], Enrico Mastrobattista[a,*]

[a] Department of Pharmaceutical Sciences, Utrecht Institute for Pharmaceutical Sciences (UIPS), Faculty of Science, Utrecht University, Utrecht, the Netherlands
[b] Drug Sector, Saudi Food and Drug Authority, Riyadh, Saudi Arabia
[c] Department of Chemical Biology & Drug Discovery, Utrecht Institute for Pharmaceutical Sciences, Utrecht University, Utrecht, the Netherlands
[d] Amsterdam UMC, University of Amsterdam, Department of Clinical Chemistry, Laboratory Genetic Metabolic Diseases, Amsterdam Gastroenterology & Metabolism, Amsterdam, the Netherlands
[e] Department of Endocrinology and Metabolism, Academic Medical Center, Amsterdam, the Netherlands

ARTICLE INFO

Keywords:
Acid sphingomyelinase
Enzyme replacement therapy
Liposome
Lysosomal storage disease
Niemann-Pick disease
Rare disease

ABSTRACT

Niemann-Pick disease type B is a hereditary rare condition caused by deficiency of the acid sphingomyelinase (ASM) that is needed for lysosomal hydrolysis of sphingomyelin to ceramide and phosphocholine. This deficiency leads to a massive accumulation of sphingomyelin in cells throughout the body, predominantly in the liver, spleen and lungs. Currently, there is no effective treatment available. Olipudase alfa (recombinant human acid sphingomyelinase; rhASM) is an investigational drug that has shown promising results. However, dose-dependent toxicity was observed in mice upon the intravenous administration of rhASM, potentially due to the systemic release of ceramide upon the extracellular degradation of sphingomyelin by rhASM. Using a nanocarrier to deliver the rhASM to cells could improve the therapeutic window by shielding the rhASM to prevent the off-target degradation of sphingomyelin. For this aim, we recombinantly expressed hASM in human cells and loaded it into different liposomal formulations at a drug-to-lipid ratio of 4% (w/w). Among four formulations, the liposomal rhASM formulation with the composition DPPC:DOPS:BMP:CHOL:DiD (59:20:10:10:1 mol%) was selected because of its superiority concerning the encapsulation efficiency of rhASM (21%) and cellular uptake by fibroblasts and macrophages. The selected liposomal rhASM formulation significantly reduced the accumulated lyso-sphingomyelin in NPD-B fibroblasts by 71%, part of this effect was stimulated by the used lipids, compared to 55% when using the free rhASM enzyme. More importantly, the undesired extracellular degradation of sphingomyelin was reduced when using the selected liposomal rhASM by 61% relative to the free rhASM. The presented *in vitro* data indicate that the liposomal rhASM is effective and may provide a safer intervention than free rhASM.

1. Background

Acid sphingomyelinase (ASM or aSMase) (EC 3.1.4.12) is an enzyme encoded by the *SMPD1* gene that catalyses the hydrolysis of sphingomyelin into ceramide and phosphocholine in response to different stimuli [1]. Niemann-Pick disease (NPD) types A and B are caused by specific mutations in the SMPD1 gene that result in the absence of (type A) or markedly decreased (type B) ASM activity [1,2]. This leads to a progressive build-up of undegraded sphingomyelin in the lysosomes of cells, particularly phagocytic mononuclear cells [3]. In NPD type A (infantile form), the clinical manifestations appear during infancy and are characterised mainly by hepatosplenomegaly, failure to thrive and the rapid progression of neurodegenerative diseases, resulting in a life expectancy of less than three years [1]. NPD type B (NPD-B) encompasses a wide spectrum of disease manifestations ranging from severe hepatosplenomegaly in patients who survive beyond early childhood to minimal involvement in adults. Those at the severe end of the spectrum also frequently have neurological involvement [1,2,4]. Types A and B NPD have a combined prevalence of 1 in 250,000 which therefore considered as ultra-rare diseases [5]. Currently, there is no specific treatment available for either NPD type A nor B. The provided medical interventions are symptomatic and supportive, such as bone

* Corresponding author.
E-mail address: e.mastrobattista@uu.nl (E. Mastrobattista).

https://doi.org/10.1016/j.ejpb.2019.02.019
Received 1 August 2018; Received in revised form 25 December 2018; Accepted 23 February 2019
Available online 25 February 2019
0939-6411/

marrow transplantation and splenectomy [2]. Olipudase alfa is a recombinant human acid sphingomyelinase (rhASM) developed as enzyme replacement therapy (ERT) for the treatment of acid sphingomyelinase deficiency (ASMD) in patients without neurologic manifestations [6]. Clinical trials are ongoing in patients with NPD type B to evaluate the safety and efficacy of olipudase alfa [7–9]. During the preclinical studies of olipudase alfa, severe toxicity in mice upon the intravenous injection of rhASM at high doses (≥10 mg/kg) was reported, which led to several adverse reactions such as cardiovascular shock, elevations in ceramide and death. Increasing the dose slowly could abrogate the toxicity, but the maximum tolerated dose was lowered to 3 mg/kg [10]. The observed toxicity was due to the rapid breakdown of the sphingomyelin in circulating lipoproteins and on the outer surface of cell membranes into ceramide. Ceramide functions as a signalling intermediate and stimulates cytokine release and cell apoptosis, which caused several adverse effects [10–14]. A phase 1b clinical trial (Identifier: NCT02004704) with five patients with ASMD type B showed promising results over 30 months of treatment at a dose of 3 mg/kg, with frequent mild adverse events [6]. In one patient, the dose had to be lowered to 1 mg/kg due to sustained adverse events [6]. The potential toxicity caused by the direct intravenous administration of rhASM may narrow the therapeutic window.

RhASM is a glycoprotein containing mannose 6-phosphate (M-6-P) and mannose residues present on carbohydrate chains [15,16]. In wild-type cells, free rhASM is internalised via M-6-P and mannose receptors on the cell surface; however, M-6-P receptors have been reported to be deficient in macrophages of ASM knock-out mice and fibroblasts of type-A NPD patients, which may limit the efficient delivery of rhASM to these cells [16,17]. The loading of rhASM into poly(lactic-co-glycolic acid) (PLGA) nanocarriers targeting intercellular adhesion molecule-1 (ICAM)-1 improved the delivery of rhASM compared to free rhASM and restored the impaired clathrin-mediated endocytosis in NPD type-A fibroblasts (derived from patients) [17,18]. However, using PLGA to deliver proteins could lead to the instability and/or denaturation of proteins due to the formation of acidic products that can dramatically lower the pH inside the PLGA matrix upon hydrolytic degradation [19,20].

Conventional liposomes – that is liposomes without a layer of poly (ethylene glycol) – are known to be taken up efficiently and rapidly by mononuclear phagocytes, which are the target cells in patients with ASMD, after intravenous (*iv*) administration [16,21–23]. For example, in rats, the *iv*-injected dose of phosphatidylserine-containing liposomes was distributed into the liver and spleen by 73% and 10%, respectively, after two hours. When using phosphatidylglycerol-containing liposomes, 36% and 41% of the injected dose were distributed into the liver and spleen, respectively, after four hours [24].

The rapid clearance of liposomes has been associated with opsonization of liposomes by plasma proteins [25–27]. The opsonization effect could cause destabilization or leakage of liposomal contents [26,28]. However, the degree of opsonization is influenced by several factors such as surface charge and size of liposomes, protein-lipid affinity, and hydrophobicity of liposomes [26,29,30]. Interestingly, ASM has shown an affinity to lipids which could reduce this effect. The N-terminus of the ASM contains a saposin-like domain that binds negatively charged lipids in the intra-lysosomal membrane [31,32]. One of the main lipids in the intralysosomal membrane is bismonoacylglycerophosphate (BMP) which binds to ASM via the saposin-like domain to bring the sphingomyelin headgroup (phosphocholine) to the catalytic site of ASM, enhancing its catalytic activity [31–35].

Consequently, liposomes (especially containing BMP) seem suitable for the passive targeting delivery of rhASM to affected cells. Accordingly, the objective of this study was to develop a liposomal formulation of recombinant human ASM and compare the cellular fate of these liposomal rhASM formulations with the free rhASM in wild-type (WT) fibroblasts, RAW 264.7 cells and NPD-B fibroblasts. To this end, we have produced human ASM in HEK293S GNT1(-) cells. The purified rhASM was encapsulated in liposomes with different lipid compositions. Liposomal formulations were characterised in terms of total rhASM loading, encapsulation efficiency of rhASM, enzymatic activity of rhASM and the colloidal stability of liposome dispersions. The liposomal formulations were tested *in vitro* for cellular uptake. Finally, the suitable liposomal formulation in terms of enzyme encapsulation and colloidal stability was tested for sphingomyelin conversion.

2. Materials and methods

2.1. Biological and chemical materials

The pcDNA3.1(+) vectors containing complementary deoxyribonucleic acid (cDNA) of the ASM precursor and mature forms were purchased from Genscript (Piscataway, NJ, United States). Human wild-type and NPD-B fibroblasts were derived from one donor each; both were primary cells. These cells were provided by the Department of Laboratory Genetic Metabolic Diseases, Amsterdam Medical Center (The Netherlands). The HEK293S GNT1(-) cells (CRL-11268) and RAW 264.7 cell line (TIB-71) were purchased from ATCC (Manassas, VA, United States). The 293 SFM II medium, glutaMAX (Gibco), Dulbecco's Modified Eagle medium with high glucose (DMEM high glucose), optimem reduced serum medium, Alexa fluor 488, DiD' oil, DiIC18(5) oil (1,1′-Dioctadecyl-3,3,3′,3′-Tetramethylindodicarbocyanine Perchlorate), lysotracker red DND-99 and Hoechst 33342 solution were purchased from Thermo fisher scientific (Waltham, MA, United States). Peptone primatone RL, protease inhibitor cocktail, rabbit anti-human ASM monoclonal antibody, proteinase K from Tritirachium album and D-mannose 6-phosphate disodium salt hydrate were purchased from Sigma-Aldrich (St. Louis, MO, United States). Goat anti-rabbit IgG conjugated with horseradish peroxidase was purchased from Cell Signaling Technology (Danvers, MA, United States). Linear polyethyleneimine, or PEI, with a molecular weight (Mwt) of 25,000 Da, was purchased from Polysciences Europe GmbH (Hirschberg an der Bergstrasse, Germany). 6-Hexadecanoylamino-4-methylumbelliferyl-phosphorylcholine (6-HMU-phosphorylcholine) and 6-Hexadecanoylamino-4-methylumbelliferone (6-HMU) were purchased from Moscerdam (Oegstgeest, The Netherlands). A strep-tactin superflow cartridge, Strep-Tactin purification buffer set and anti-Twin-Strep-tag conjugated with horseradish peroxidase were purchased from IBA GmbH (Göttingen, Germany). Moreover, 16:0 1,2-dipalmitoyl-*sn*-glycero-3-phosphocholine (DPPC), 18:1 1,2-dioleoyl-*sn*-glycero-3-phospho-L-serine (DOPS), 18:1 bis(monooleoylglycero)phosphate (S, R Isomer) (BMP), cholesterol (CHOL) and 16:0 1,2-dipalmitoyl-*sn*-glycero-3-phospho-(1′-*rac*-glycerol) (DPPG) were purchased from Avanti (Alabaster, AL, United States). Ham's F12 medium was purchased from Lonza (Basel, Switzerland).

2.2. Protein expression and purification

The cDNA of ASM precursor and mature forms were generated and cloned into pcDNA3.1(+) vectors by Genscript and subsequently subcloned into pCD5 vectors (Fig. S1) [36]. Both ASM precursor and mature forms contained either an N- or C- terminal fusion with a seven amino-acid cleavage recognition sequence (ENLYFQG) of tobacco etch virus (TEV), a Superfolder GFP (sfGFP) and a Twin-Strep-tag (WSHPQFEK-(GGGS)2-GGS-SA-WSHPQFEK) adapted from (Table 1) [36].

Subsequently, pCD5 expression vectors were transfected into HEK293S GNT1(-) cells with polyethyleneimine I (PEI) at a 1:5 ratio (μg DNA: μg PEI). After six hours, the transfection mix was replaced with 293 SFM II medium only (original medium) or supplemented with glucose 2.0 g/L, sodium bicarbonate 3.6 g/L, primatone 3.0 g/L, 1% glutaMAX, 1.5% DMSO and 2 mM valproic acid (enriched medium). Culture supernatants were harvested five days post-transfection and assessed using Western blot analysis.

Table 1
The order of DNA inserts within the reading frame of the pCD5 vector.

Used expression vector	Order of DNA inserts within reading frame				Expression plasmid abbreviation	Recombinant protein abbreviation	*pI*	Mwt (kDa)
	1	2	3	4				
pCD5	S	G	TEV	p	pCD5/S-G/p-rhASM	S-G/p-rhASM	6.51	109
pCD5	p	TEV	G	S	pCD5/p-rhASM/G-S	p-rhASM/G-S	6.51	109
pCD5	S	G	TEV	m	pCD5/S-G/m-rhASM	S-G/m-rhASM	6.51	106
pCD5	m	TEV	G	S	pCD5/m-rhASM/G-S	m-rhASM/G-S	6.51	106

pI: isoelectric point; Mwt: molecular weight: S: twin-Strep-tag; G: superfolder GFP; TEV: tobacco etch virus; p: precursor form; m: mature form. Note: The Mwt includes sizes of seven N-linked glycosylation sites, 2 kDa per site on average [37,38].

For large-scale production, the previously described procedure was followed. Next, the supernatant was harvested and centrifuged at 4427 × *g* at 4 °C then micro-filtered using a 0.2 μm mPES MidiKros hollow fibre filter connected to an automated Krosflo research II Tangential flow filtration (TFF) system (Repligen, Waltham, Massachusetts, USA). The flow-through was ultra-filtrated through mPES MidiKros hollow fibre filter with molecular weight cut-off of 30 kDa. The retentate containing the rhASM was analysed using SDS-PAGE and Western blot.

For large scale production, affinity chromatography was used to purify p-rhASM/G-S utilising a Strep-Tactin superflow cartridge (5 mL) connected to AKTA purifier (GE, Boston, MA, United States) according to the manufacturer's protocol. The elution fractions were analysed using SDS-PAGE and enzyme activity.

2.3. Western blot

The samples were diluted to the same protein concentration and prepared according to the manufacturer's protocol of bolt 4–12% Bis-Tris Plus gels (Thermo Fisher Scientific). The gel was removed from the cassette, and the proteins were transferred to an immun-blot PVDF membrane (Bio-Rad Laboratories, Hercules, CA, USA) using the Trans-Blot Turbo Transfer System (Bio-Rad Laboratories). After the transfer, the membrane was incubated in phosphate-buffered saline (PBS) with 0.05% Tween 20 and 1% bovine serum albumin (blocking buffer) overnight at 4 °C with continuous agitation. The membrane was incubated with rabbit anti-human ASM monoclonal antibody (1:100 in blocking buffer) or anti-Twin-Strep-tag antibody (1:2000 in blocking buffer) overnight at 4 °C with continuous agitation. The membrane was washed three times using PBS with 0.05% Tween 20 for five minutes each. The membrane was incubated with goat anti-rabbit IgG conjugated with horseradish peroxidase (1:1000 in blocking buffer) overnight at 4 °C with continuous agitation. Again, the membrane was washed three times using PBS with 0.05% Tween 20 for five minutes each. The Supersignal West Pico PLUS Chemiluminescent Substrate (Thermo Fisher Scientific) was used for detection.

2.4. Enzyme activity assay

The artificial substrate (6-HMU-phosphorylcholine) was prepared at a concentration of 0.68 mM in 100 mM sodium acetate buffer, pH 5.2, with 0.2% (w/v) sodium taurocholate (substrate buffer). Before use, the substrate was heated to 37 °C briefly. A black 96-Well Half-Area Plate with flat bottom (Greiner Bio-One, Austria) was used for the assay. All tests were performed in duplicate. For the end-point assay, 10 μL of the substrate and 30 μL of a sample (10 μg or unless otherwise stated) were added into a well and incubated at 37 °C for one hour. The reaction was halted by adding 150 μL of 500 mM sodium carbonate buffer, pH 10.7, with 0.25% (w/v) Triton X-100 (stop buffer). Fluorescence was measured using an FP-8300 Spectrofluorometer (Jasco, Easton, MD, United States) at an excitation wavelength of 404 nm and emission wavelength of 460 nm. For a kinetic assay, 10 μL of the substrate and 30 μL of pure rhASM (42 ng, unless otherwise stated) in the substrate buffer were added into a well and incubated at 37 °C. The reaction was stopped by adding 150 μL of stop buffer at time points 0, 30 min, 60 min, 90 min and 120 min. Fluorescence was measured using the described measurement settings in an end-point assay. A calibration curve was prepared using 6-HMU in a linear concentration range of 0–6.3 nM (10 measurement points). Specific enzyme activity was determined by calculating the best-fit slope.

2.5. Selection and preparation of liposomal formulations

DPPC, DOPS and BMP were dissolved in chloroform (25 mg/mL each) separately. DPPG was dissolved in a 1:5 (v/v) mixture of methanol and chloroform at 2 mg/mL. DiD was dissolved in methanol at 200 μg/mL. The compositions and molar ratios of the liposomal formulations are shown in Table 2.

All liposomal formulations were prepared at a total lipid concentration of 25 mM. For each liposomal formulation, non-loaded and loaded liposomes were prepared. Since the sfGFP signal was undetectable when using confocal imaging microscopy, p-rhASM/G-S was labelled using Alexa fluor 488 (dye) at a ratio of 8 p-rhASM/G-S:1 dye in 0.1 M sodium bicarbonate buffer, pH 8.3. The mixture was subjected to constant rotation for one hour at room temperature and protected from light. The non-conjugated dye was removed using a spinning column with a 10 kDa MWCO filter (Vivaspin, GE). The filter was washed with PBS and centrifuged for 20 min at 4362 × *g* and 4 °C for five times. The labelled p-rhASM/G-S was analysed using HPLC with an SRT-C SEC-150 column (Newark, DE, United States), and the degree of labelling was determined using a Nanodrop (ND-1000 Spectrophotometer, Thermo Fisher Scientific).

The thin-film hydration (TFH) method was used to prepare the PS liposomal formulation for p-rhASM/G-S with a drug-to-lipid (D/L) ratio of 1% (w/w) [39]. The dried-reconstituted vesicles (DRV) method was used to prepare a PS liposomal formulation with a D/L of 1% (w/w); in addition, PS, PS-BMP, PG and PG-BMP liposomal formulations with a D/L of 4% (w/w) were prepared using the DRV [40].

The liposomal formulations from both LFH and DRV methods were extruded through a 200 nm diameter size using a mini extruder (Avanti) and washed by ultracentrifugation at 187,360 × *g* and 4 °C for 60 min. The liposomal pellets were resuspended in 50 mM HEPES buffer pH 7.4 with 0.9% NaCl (formulation buffer) with gentle rotation at 4 °C overnight. The ultracentrifugation step was repeated. The volume of each liposomal formulation was adjusted to 1 mL with the formulation buffer. The hydrodynamic diameter and surface charge were measured using Zetasizer Nano S and Zetasizer Nano Z, respectively (Malvern

Table 2
Compositions and molar ratios of the prepared liposomal formulations.

Formulation composition	Molar ratio (%)	Liposomal formulation abbreviation
DPPC:DOPS:CHOL:DiD	69:20:10:1	PS
DPPC:DOPS:BMP:CHOL:DiD	59:20:10:10:1	PS-BMP
DPPC:DPPG:CHOL:DiD	69:20:10:1	PG
DPPC:DPPG:BMP:CHOL:DiD	59:20:10:10:1	PG-BMP

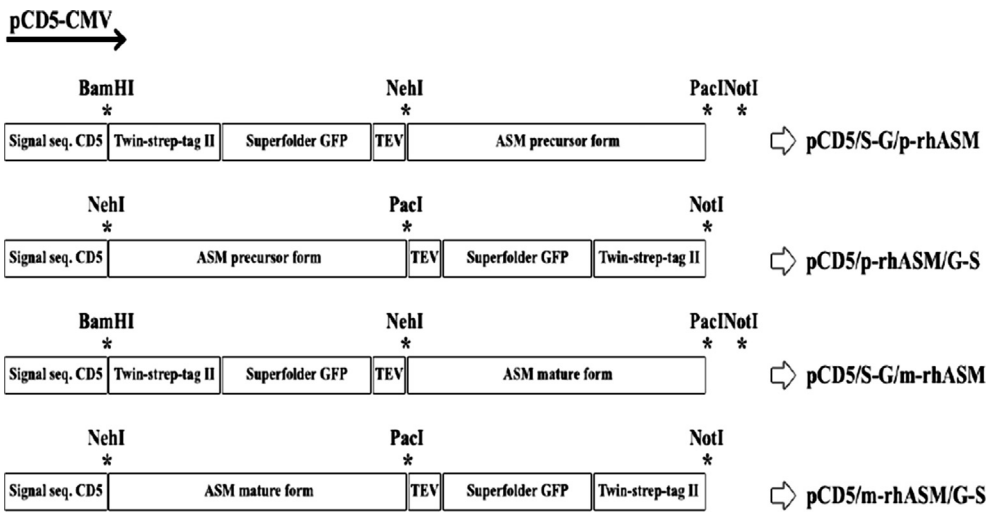

Fig. 1. Schematic representation of the gene constructs encoding the precursor or mature form of human ASM fused to Superfolder GFP for detection and Twin-Strep-tag for purification. pCD5: CD5 vector; CMV: human cytomegalovirus immediate early enhancer/promoter; black arrow: direction of reading; seq.: sequence; *: restriction enzyme cleavage site; TEV: tobacco etch virus protease recognition site.

Panalytical, United Kingdom). The phospholipid amount was determined using the Rouser method [41]. The loading efficiency, encapsulation efficiency and loading capacity were determined directly after the preparation. The enzyme activity of incorporated p-rhASM/G-S was determined using 150 ng as the total protein amount.

2.5.1. Determination of enzyme loading efficiency and capacity of liposomal formulations

The amount of rhASM that can be loaded in and onto the liposomes (encapsulated and surface bound) was determined after the removal of free rhASM from liposomes using ultracentrifugation (washed twice at 187,360 × g). RhASM was extracted from liposomes using the Bligh and Dyer extraction method with some modifications [42]. The initial rhASM amount that was loaded into liposomes was used as a control (100%). The following was added to 120 µL of a sample in the same order: four parts methanol, one part chloroform and three parts water. The mixture was vortexed after each addition. The mixture was centrifuged for 15 min at 18,335 × *g*. The top aqueous layer was removed without disturbing the middle flake layer. Three parts of methanol and a half-part of 20 mM of ammonium sulfate were added and vortexed briefly, then centrifuged for 30 min at 18,335 × *g*. The liquid layer was removed, and 60 µL of 1% SDS with 20 mM NaOH was added to the pellet, vortexed briefly and incubated at 50 °C for five minutes. The protein concentration was determined using a Pierce BCA Protein Assay Kit (Thermo Fisher Scientific). The loading efficiency (%LE) was calculated from the 100% control using the following formula:

$$\%LE = [\text{calculated protein amount } (\mu g) \text{ present in or on the liposomes} / \text{initial protein amount } (\mu g) \text{ that was added to the liposomes}] * 100) \quad (1)$$

After the determination of the phospholipid amount of liposomal formulations, the loading capacity (%LC) was calculated as follows:

$$\%LC = [\text{calculated protein amount in or on the liposomes } (\mu g) / \text{calculated phospholipid amount of the liposome } (\mu g)] * 100) \quad (2)$$

2.5.2. Determination of encapsulation efficiency of liposomal formulation

After determining the amount of rhASM in the liposomal formulations, proteinase K was added to the loaded liposomes at a weight ratio of 2 proteinase K: 1 rhASM in 50 mM Tris-HCl (pH 8) and 10 mM $CaCl_2$. The loaded liposomes without proteinase K were included as controls. All mixtures were incubated at 40 °C for two hours. An end-point enzyme activity assay was performed. The encapsulation efficiency (%EE) was determined as follows:

$$\%EE = [\text{number of fluorescence units of the liposomal formulation with proteinase K} / \text{number of fluorescence units of the liposomal formulation without proteinase K}] * \%LE) \quad (3)$$

For the subsequent evaluation of these formulations on cells, the labelled p-rhASM/G-S and loaded liposomal formulations were diluted to a protein concentration of 250 µg/mL. Next, the non-loaded liposomal formulations were diluted to the same lipid concentration of the corresponding loaded liposomal formulations.

2.6. Cellular uptake of rhASM

Wild-type fibroblasts, NPD-B fibroblasts (derived from a patient) and RAW 264.7 cells were seeded at cell densities of 5000, 5000 and 20,000 cells per well, respectively, with 150 µL of DMEM high glucose with 10% FBS (one plate per each cell type). The black µ-clear 96-well plate with flat bottom (Greiner, The Netherlands) was used. The cells were incubated overnight in a humidified CO_2 incubator at 37 °C and 5% CO_2 (incubation conditions for cells). The next day, the culture medium was replaced with fresh medium for fibroblasts and RAW 264.7 cells, respectively. For fibroblasts, 20 µL (or 1 µg for the formulation with enzyme) of each tested formulation was added to wells in triplicate. For RAW 264.7 cells, 4 µL (or 1 µg for the formulation with enzyme) of each tested formulation was added to wells in triplicate. The plates were incubated for four hours, and then the medium was replaced with 150 µL of DMEM (without phenol red) with 10% FBS and 100 nM of lysotracker red for WT fibroblasts and RAW 264.7 cells or 50 nM of lysotracker red for NPD-B fibroblasts. The plates were incubated for 30 min, and the medium was replaced with 150 µL of DMEM with 10% FBS (without phenol red) and 40 µM of Hoechst 33342 solution and incubated for 20 min. The cells were washed once with the medium, and 150 µL of DMEM with 10% FBS (without phenol red) was added. Confocal microscopy (Cell Voyager 7000S, Yokogawa Europe B.V., The Netherlands) was used for the cell imaging. Confocal images were assessed with Columbus Image Data Storage and Analysis System (PerkinElmer, Waltham, Massachusetts, United States) using automated segmentation protocols for nuclei and cytoplasm detection and built-in functionalities for the determination of average fluorescence intensity and the calculation of Pearson's correlation coefficient.

2.7. Cellular activity of rhASM

The WT and NPD-B fibroblasts were cultured in a 24-well plate at a

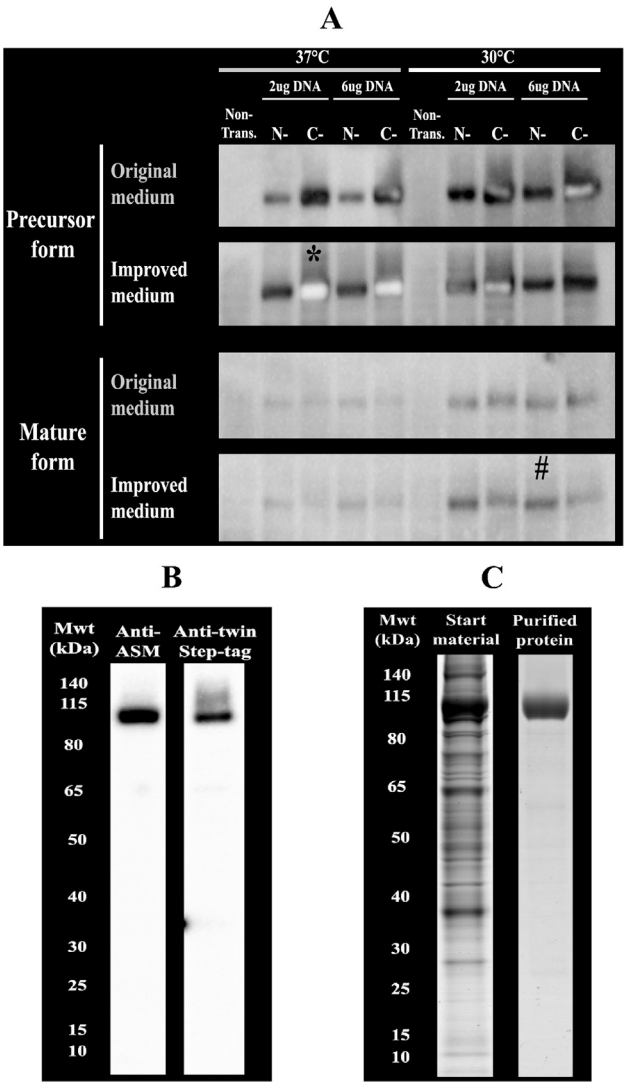

Fig. 2. A. Western blot analysis using the anti-Twin-Strep-tag antibody to detect rhASM in HEK293S GNT1(-) cell culture supernatants at different conditions. Non-trans.: non-transfected; N-: rhASM with fusion proteins on the N-terminus; C-: rhASM with fusion proteins on the C- terminal; Original medium: 293 SFM II medium; Enriched medium: 293 SFM II medium supplemented with 3 g/L peptone primatone RL, 3.7 g/L sodium bicarbonate, 2 g/L glucose, 1% glutaMAX, 1.5% DMSO and 2 mM valproic acid. *: highest protein expression for precursor form. #: highest protein expression for mature form. Note: 10 µg of PEI was used in each tested condition. The white protein band indicates a high signal due to high protein/antibody concentration. B. Western blot analysis of cell culture supernatant using anti-ASM and anti-Twin-Strep-tag antibodies; C. SDS-PAGE (Coomassie Brilliant Blue staining) of cell culture supernatant before and after purification.

cell density of 200,000 cells per well for two days with 500 µL of Ham's F12 medium and 10% FBS. On the third day, the culture medium was replaced with fresh medium. For WT fibroblasts, 40 µL of the formulation buffer was added per well and incubated for four hours. For NPD-B fibroblasts, 40 µL (or 10 µg for the formulation with enzyme) of each formulation, free p-rhASM/G-S and PS-BMP liposomes (non-loaded and loaded) was added per well and incubated for four hours. The cells were washed once. Subsequently, 150 µL of 1x trypsin and 1x protease cocktail inhibitor were added, and the plate was incubated for 30 min. The cells were collected and sonicated for one minute in an ultrasonic bath (FB 15046, Fisher Scientific, Waltham, MA, United States) and subjected to three cycles of freeze-thawing. The protein concentrations of the cell lysates were normalised to 0.4 mg/mL. ASM

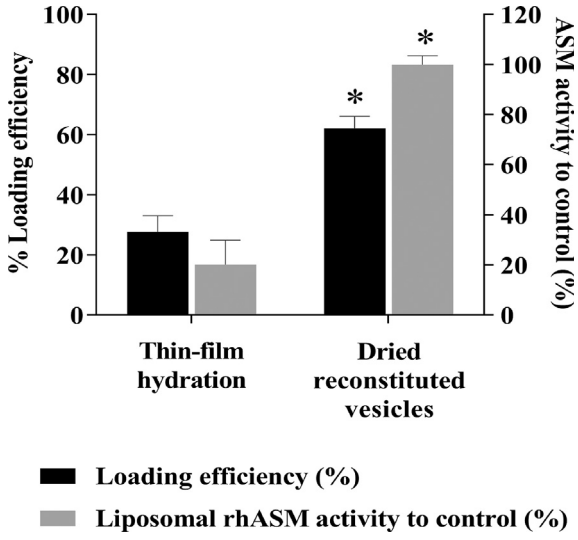

Fig. 3. Loading efficiency and enzyme activity of p-rhASM/G-S loaded in the PS liposomes using different formulation methods. Data represent the mean (± SD) of two independent samples, each performed in duplicate. *: $p < 0.05$ (comparison with thin-film hydration).

activity in the cell lysates was measured using the end-point enzyme activity assay.

2.8. Reduction of accumulated lipids

The WT and NPD-B fibroblasts were cultured in a six-well plate format at cell densities of 400,000 cells per well for five days with 3 mL of Ham's F12 medium and 10% FBS. On the sixth day, the culture medium was replaced with 2920 µL of fresh medium. For WT fibroblasts, 80 µL of formulation buffer was added per well in duplicate and incubated for four hours. For NPD-B fibroblasts, 80 µL (or 20 µg for the formulation with enzyme) of each formulation buffer, free p-rhASM/G-S and PS-BMP liposomes (non-loaded and loaded) were added per well in duplicate and incubated for four hours. The cells were washed once, and 3 mL of fresh culture medium was added. The cells were incubated overnight. On the next day, the medium was removed. Then, 250 µL of 1x trypsin and 1x protease cocktail inhibitor were added. The plate was incubated for 30 min. The cells were collected and sonicated for one minute in an ultrasonic bath and subjected to three cycles of freeze-thawing. The protein concentrations of the cell lysates were normalised to 0.4 mg/mL. The lyso-sphingomyelin amount in the cell lysate was determined as previously described [43].

2.9. Fluorometric sphingomyelin degradation assay

The Fluorometric Sphingomyelin Assay Kit (Sigma-Aldrich) was used to determine the relative amount of converted sphingomyelin by p-rhASM/G-S and PS-BMP liposomes (non-loaded and loaded).

2.10. Statistical analysis

Data were analysed using GraphPad Prism 7.04 for Windows (GraphPad Software, La Jolla, CA, USA). Data are presented as means ± standard deviations (SD). Comparative analyses were performed using the analysis of variance (ANOVA). For all statistical comparisons, a value below 0.05 was considered statistically significant.

Table 3
Characteristics of prepared liposomal formulations.

Liposomal formulation and composition	Type	Hydro-dynamic diameter (nm)	Zeta potential (mV)	D/L% (w/w)	LE (%)	EE (%)	Enz. act. (%)[a]
PS	Non-loaded	187 ± 3.0	−17 ± 1.3	–	–	–	–
(DPPC:DOPS: CHOL:DiD) (69:20:10:1mol%)	Loaded	187 ± 4.4	−19 ± 1.3	1.9 ± 0.0	48 ± 0.7	14 ± 0.0	99.5 ± 2.1
PS-BMP	Non-loaded	186 ± 1.9	−27 ± 1.6	–	–	–	–
(DPPC:DOPS: BMP:CHOL:DiD) (59:20:10:10:1mol%)	Loaded	184 ± 0.4	−27 ± 1.5	2.1 ± 0.1	50 ± 2.1	21 ± 2.1	104.0 ± 7.1
PG	Non-loaded	184 ± 0.1	−23 ± 1.2	–	–	–	–
(DPPC:DOPS: CHOL:DiD) (69:20:10:1mol%)	Loaded	174 ± 4.2	−25 ± 0.7	3.8 ± 0.1	55 ± 0.7	7 ± 0.0	44.0 ± 4.2[b]
PG-BMP	Non-loaded	197 ± 1.6	−28 ± 1.1	–	–	–	–
(DPPC:DPPG: BMP:CHOL:DiD) (59:20:10:10:1mol%)	Loaded	206 ± 0.5	−27 ± 0.8	2.7 ± 0.0	56 ± 1.4	8 ± 0.0	94.0 ± 2.8

D/L: drug-to-lipid ratio; LE: loading efficiency (encapsulated and surface bound); EE: encapsulation efficiency. Data represent the mean (± SD) of a duplicate of one sample.

[a] Enz. act. (%): Enzyme activity of loaded liposome/Enzyme activity of p-rhASM/G-S (Control) * 100.

[b] The determination may be influenced by the incomplete access of artificial substrate to p-rhASM/G-S.

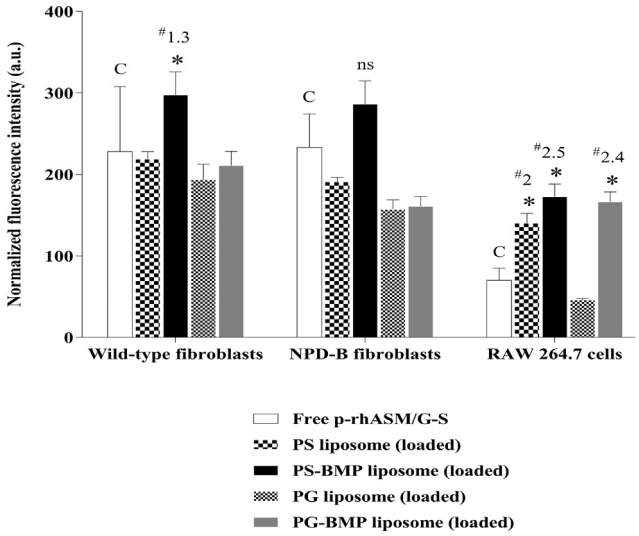

Fig. 4. Quantitative analysis of the binding and uptake of labelled p-rhASM/G-S as free enzymes or in liposomal formulations by wild-type fibroblasts, NPD-B fibroblasts (derived from a patient) and RAW 264.7 cells after four hours' incubation. The value per well was normalised to the vehicle (50 mM HEPES buffer, pH 7.4, with 0.9% NaCl). Data represent the mean (± SD) of three independent samples, each measured one time. Average numbers of analysed cells were 216 cells (± 45 SD) for wild-type fibroblasts, 108 cells (± 28 SD) for NPD-B fibroblasts and 1961 cells (± 167 SD) for RAW 264.7. C: control; ns: not significant; *: $p < 0.05$ (comparison with C); #: fold increase in uptake relative to free p-rhASM/G-S. 5 µg and 1 µg of labelled p-rhASM/G-S were used for fibroblasts and RAW 264.7 cells, respectively.

3. Results and discussion

3.1. Protein expression and purification

Human acid sphingomyelinase is synthesised as a 75 kDa propolypeptide then glycosylated and processed in the endoplasmic reticulum and Golgi apparatus before being sorted into lysosomes as a 70 kDa mature form or secreted extracellularly as a 75 kDa precursor form [15].

In this study, the mature form (m-rhASM) and precursor form of ASM (p-rhASM) were recombinantly produced. The m-rhASM was used for encapsulation into liposomes for direct lysosomal delivery. Meanwhile, p-rhASM was used as a control mimicking the uptake mechanism of the ERT approach, in which the precursor form is delivered to lysosomes via the mannose-6-phosphate uptake pathway, where it is converted into the mature form [44,45].

The amino acid sequences of precursor and mature forms were reported to start from His60 and Gly83, respectively, of the full-length ASM; these sequences were used to generate cDNAs (Fig. S1) [46,47].

The pCD5 vector was used for protein expression with the signal sequence of the CD5 protein to guide the recombinant protein into the secretory pathway [48]. The coding sequence for p-rhASM or m-rhASM was fused to Superfolder GFP and Twin-Strep-tag, with protease cleavage sites in between, as illustrated in Fig. 1.

The plasmid constructs were transfected into HEK293S GNT1(-) cells at different conditions (DNA: PEI ratio, temperature, culture medium) to select favourable conditions for high protein expression. Western blot analysis showed that the highest protein band intensity (suggesting high protein expression) was for the rhASM precursor form with the Superfolder GFP and Twin-Strep-tag appended to the C-terminus (p-rhASM/G-S) using a ratio of 2 DNA:10 PEI and feeding the cells with enriched culture medium at 37 °C (Fig. 2A). Notably, the rhASM mature form has a very low expression level (maximum ~0.4 mg/mL) compared to the rhASM precursor form (maximum ~4 mg/L), despite the use of identical plasmids. However, they differed in the starting position of the amino acid sequence, which could influence the protein expression (Fig. S2).

Due to the low expression of the mature form of rhASM and slight difference in the specific enzyme activity of the rhASM precursor and mature forms, the rhASM precursor form with fusion proteins on the C-terminus (p-rhASM/G-S) was selected for further steps (Fig. S3). The p-rhASM/G-S fusion protein has a molecular weight of ~109 kDa (75 kDa without fusion proteins) [49]. The identity of rhASM/G-S and presence of Twin-Strep-tag were confirmed using Western blot analysis before protein purification was initiated (Fig. 2B). Affinity chromatography using Strep-Tactin resin was performed to capture the Twin-Strep-tag appended to the C-terminus of p-rhASM/G-S. SDS-PAGE was performed before and after purification to compare the protein purity profile (Fig. 2C). Purified p-rhASM/G-S has a protein purity of > 90% after a single affinity chromatography step, with a yield of 4 mg/L. The specific enzyme activity of pure p-rhASM/G-S was determined at 21.6 mmol/hour/mg using the substrate (6-HMU-phosphorylcholine). The purified protein was stored at −80 °C to preserve enzyme activity until it was used for liposomal formulation.

3.2. Selection and preparation of liposomal formulations

3.2.1. Selection of lipid composition and formulation method for liposomal rhASM

The proper selection of lipid composition for liposomes is crucial to

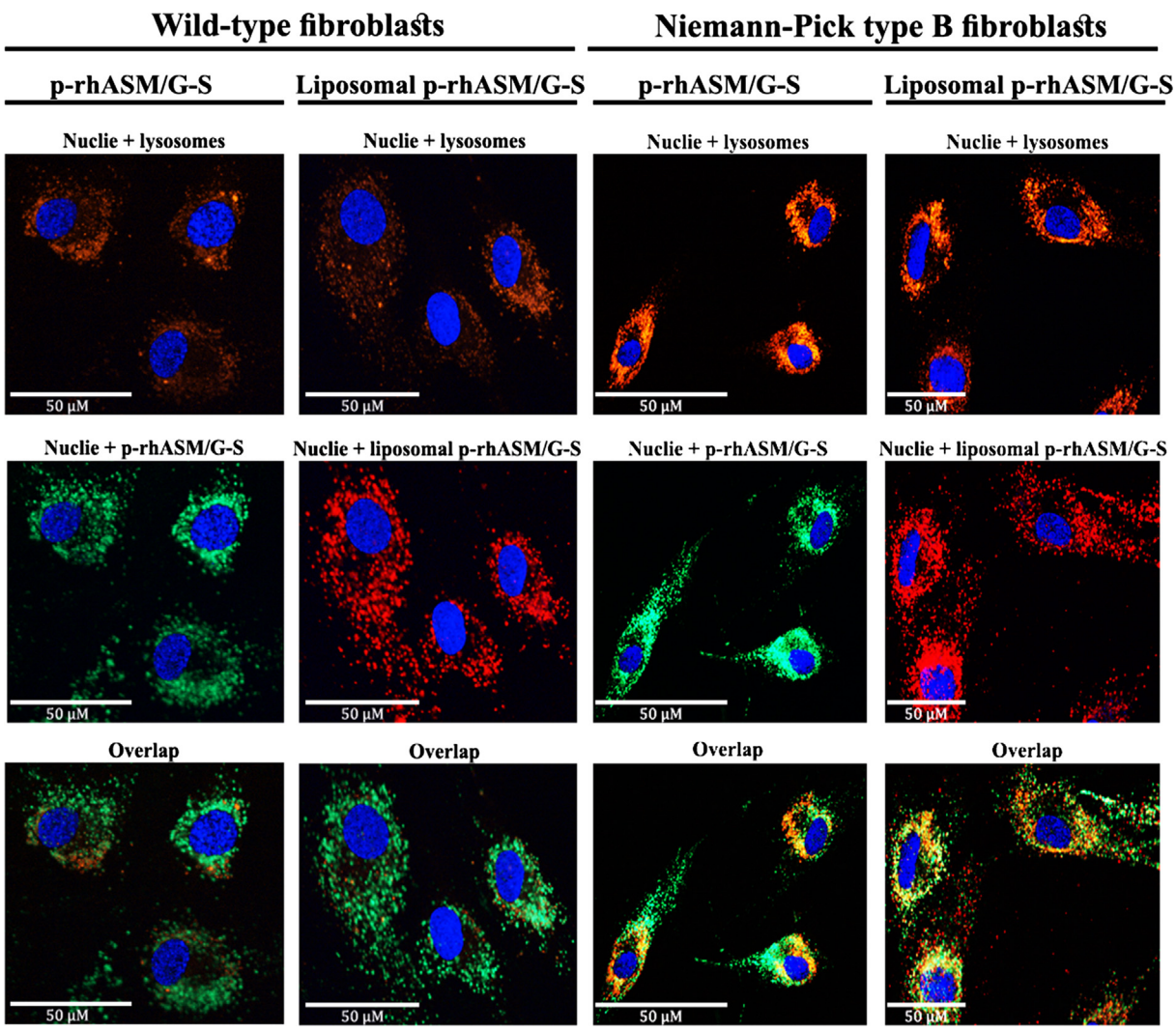

Fig. 5. Confocal images of the cellular uptake of free p-rhASM/G-S and PS-BMP liposomal p-rhASM/G-S by wild-type and Niemann-Pick type B fibroblasts. Nuclei, lysosomes, p-rhASM/G-S, and liposomes are stained in blue, orange, green, and red, respectively. Bar size is 50 µm.

obtain the required properties and effects. In this study, the main selection criteria for the desired liposomes were high loading efficiency of rhASM and the passive targeting of macrophages. Reportedly, conventional liposomes containing the negatively charged phospholipids PS or PG are efficiently taken up by the liver and spleen with different uptake profiles [24]. In addition, the presence of PS or PG in liposomes at concentrations > 20 mol% enables the binding of rhASM to the liposomal surface by virtue of the N-terminal saposin-like domain, with distinct binding capacities for PS and PG [34]. Moreover, the anionic lipid BMP at concentrations > 5 mol% stimulates the degradation of sphingomyelin by ASM and has a higher binding affinity to ASM than PS [31,34].

Therefore, liposomal formulations containing either PS or PG are expected to exhibit variations in the loading efficiency of rhASM and cellular uptake. The use of BMP could improve the loading efficiency of rhASM and stimulate the degradation of sphingomyelin; however, the effect on cellular uptake cannot be predicted due to the scarcity of data. Given the above, four liposomal formulations with assorted compositions and molar ratios were investigated respecting their influences on the properties of liposomes and *in vitro* behaviour (Table 2).

For the proper loading of p-rhASM/G-S into liposomes, the TFH and DRV formulation methods were investigated using one of the proposed liposomal formulations (PS liposomal formulation) (Table 2) [39,40]. At 1% (w/w) enzyme-to-lipid ratio, a high enzyme loading efficiency (62%), defined as the amount of enzyme bound to or encapsulated in the liposomes, was achieved with the DRV method compared to the TFH method (28%) (Fig. 3). The high loading efficiency obtained with the DRV method can be ascribed to the high lipid concentration (125 mM) and large exposed surface area upon hydration with the enzyme (p-rhASM/G-S) solution. Moreover, a significant decrease in the recovered enzyme activity (20%) was observed after the preparation of liposomes using the TFH method. The reason for this observation was the use of relatively high temperature (46 °C) to hydrate the lipid film, which was detrimental to the enzymatic activity (Fig. 3). Based on these findings, the DRV method was chosen as a suitable formulation method to prepare the four liposomal formulations (Table 2).

3.2.2. Preparation of liposomal formulations

The PS, PS-BMP, PG and PG-BMP liposomal formulations (non-loaded and loaded) were prepared using the DRV method. Their hydrodynamic diameters were determined to be between 174 and 206 nm, and zeta potentials were between −17 and −28 mV. The formulations with BMP lipids exhibited higher negative surface potentials compared to the other formulation, which was expected due to the replacement of 10 mol% of the zwitterionic DPPC with the negatively charged BMP (Table 3). The loaded PS and PS-BMP liposomal formulations showed similar D/L ratios at 1.9% and 2.1% (w/w) and similar loading efficiencies at 48% and 50%, respectively (Table 3). However, their

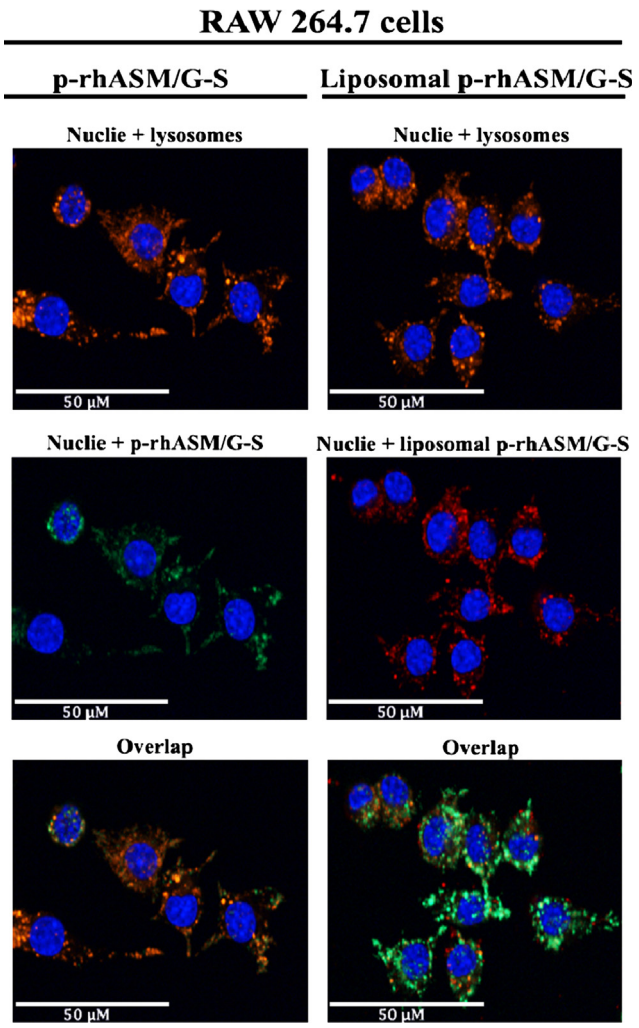

Fig. 6. Confocal images of the cellular uptake of free p-rhASM/G-S and PS-BMP liposomal p-rhASM/G-S by RAW 264.7 cells. Nuclei, lysosomes, p-rhASM/G-S, and liposomes are stained in blue, orange, green, and red, respectively. Bar size is 50 µm.

encapsulation efficiencies differed at 14% and 21%, respectively (Table 3). The loaded PG and PG-BMP liposomal formulations showed higher D/L ratios at 3.8% and 2.7% (w/w) and slightly higher loading efficiencies at 55% and 56%, respectively, compared to the PS-containing liposomes (Table 3). The high D/L ratios for the loaded PG-containing liposomes could be due to the high affinity of ASM to PG compared to PS [34]. This assumption is supported by the low encapsulation efficiencies of PG and PG-BMP formulations at 7% and 8%,

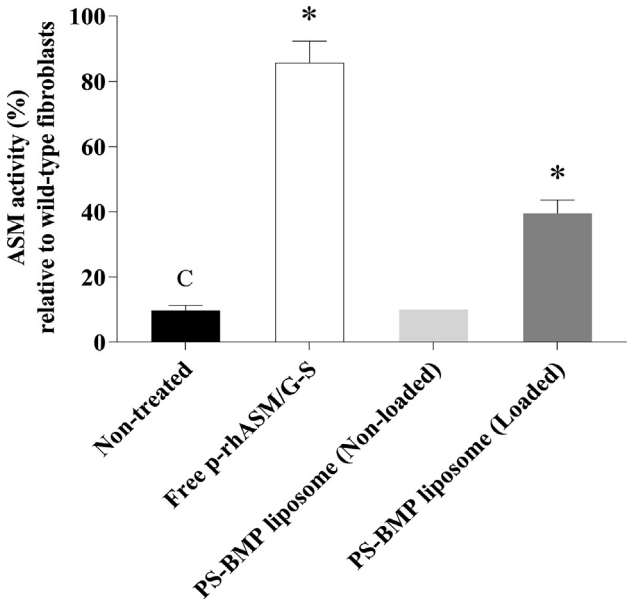

Fig. 8. Determination of ASM activity in NPD-B fibroblasts (derived from a patient) relative to ASM activity level in wild-type fibroblasts before and after treatment with free p-rhASM/G-S or liposomal formulations for four hours. Data represent the mean (± SD) of two independent samples, each performed in duplicate. C: control; *: $p < 0.05$ (comparison with C).

respectively, compared to 14% and 21% for PS and PS-BMP formulations, respectively, indicating the enzyme was bound to PG on the outer surface of liposomes (Table 3).

Notably, the addition of 10% BMP to PS-BMP liposomal formulations led to an increase in encapsulation efficiency by 50% compared to PS liposomal formulations, suggesting an increase in the molar ratio of BMP can improve the encapsulation efficiency of PS-containing liposomes for ASM.

The specific enzyme activity of liposome-incorporated p-rhASM/G-S was measured and compared to free p-rhASM/G-S enzymes. Specific enzyme activity between 94% and 104% was achieved for all loaded liposomes, except the PG liposomal formulation in which a markedly low specific enzyme activity was obtained (44%), suggesting the influence of PG on ASM activity by an unknown mechanism (Table 3). Interestingly, the specific enzyme activity of incorporated p-rhASM/G-S was fully recovered by substituting 10 mol% of DPPC for BMP lipid in PG-liposomal formulations.

Due to the presence of the unspecific phospholipase C activity of ASM that could lead to a change in the formation of liposomes, changes in the hydrodynamic diameters of the liposomal formulations were followed for one month to determine their stability when stored at 4 °C. The liposomal formulations showed no change in their hydrodynamic

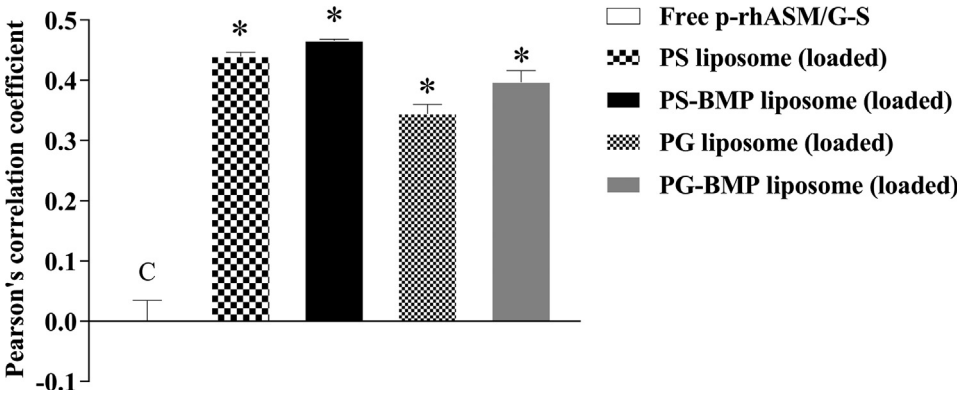

Fig. 7. Colocalisation of labelled p-rhASM/G-S (by Alexa Fluor 488) in different formulations with lysosomes (LysoTracker Red DND-99) in RAW 264.7 cells after four hours of incubation. All values were normalised to vehicle (50 mM HEPES buffer, pH 7.4, with 0.9% NaCl). Data represent the mean (± SD) of three independent samples, each measured one time. C: control; *: $p < 0.05$ (comparison with C). Average numbers of analysed cells were 1,800 cells (± 134 SD) for free p-rhASM/G-S, 1934 cells (± 22 SD) for PS liposomes, 1842 cells (± 80 SD) for loaded PS-BMP liposomes, 1934 cells (± 283 SD) for PG liposomes and 1940 cells (± 228 SD) for PG-BMP liposomes.

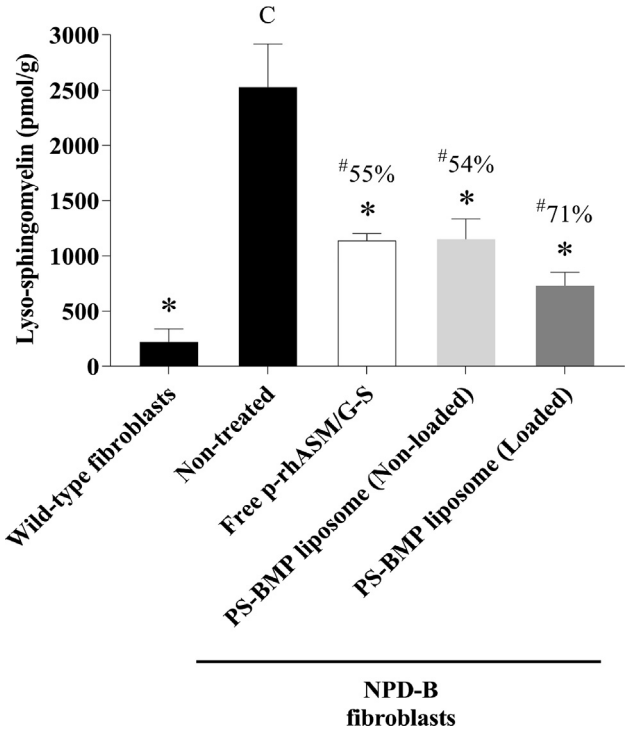

Fig. 9. Determination of lyso-sphingomyelin amount (in pmol/g of total cellular protein) in wild-type fibroblasts and NPD-B fibroblasts (derived from a patient) before and after treatment with free p-rhASM/G-S or PS-BMP liposomal formulations for four hours, followed by incubation for 20 h. Data represent the mean (± SD) of two independent samples, each performed in duplicate. #: % reduction in lyso-sphingomyelin accumulation relative to non-treated NPD-B fibroblasts; C: control; *: $p < 0.05$ (comparison with C).

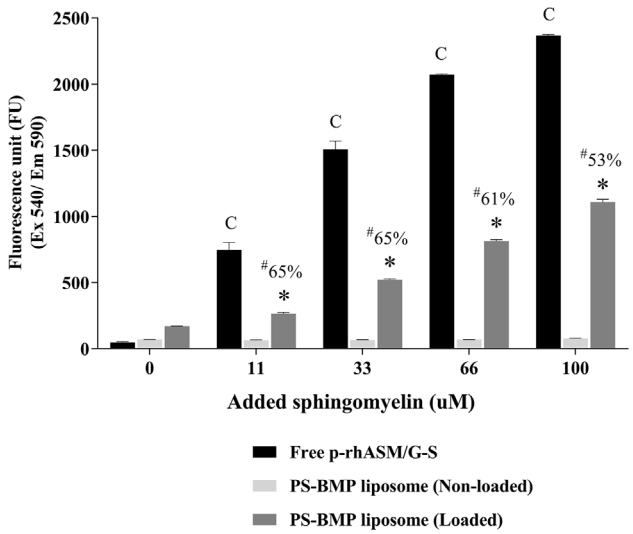

Fig. 10. Conversion of sphingomyelin by different ASM formulations after 4 h incubation. The amount of degraded sphingomyelin is directly proportional to the measured fluorescence units. Data represent the mean (± SD) of a duplicate of one sample. C: Control; #: %Reduction in sphingomyelin conversion relative to free p-rhASM/G-S. *: $p < 0.05$ (comparison with C).

diameters, except the PG-BMP formulation, which showed an increase in the hydrodynamic diameter by 11% after 10 days, with an additional increase by 5–10% until day 30 (Fig. S4).

Consequently, the prepared formulations showed differences in the incorporation of p-rhASM/G-S, and interestingly the loaded PS-BMP liposomes showed the highest encapsulation efficiency. A high encapsulation efficiency is desirable, as it will most likely minimise the systemic, off-target activity of the enzyme.

3.3. Cellular uptake of rhASM

The cellular uptake of PS, PS-BMP, PG and PG-BMP liposomal formulations was studied in various cell types and compared to the free p-rhASM/G-S enzyme, which is expected to be taken up through receptor-mediated endocytosis, such as via M-6-P receptors [16,17]. Conventional liposomes are known to be taken up through micropinocytosis, phagocytosis and receptor-mediated endocytosis (*i.e.* scavenger receptors). The uptake route followed is highly dependent on the cell type [22,50,51].

The cellular uptake of all formulations was investigated in fibroblasts. The cellular uptake of free p-rhASM/G-S in WT and NPD-B fibroblasts was similar, which is surprising, since an impairment of clathrin-mediated endocytosis in the fibroblasts of NPD type A was reported (Fig. 4) [17,18]. Among all the tested formulations, the loaded PS-BMP liposomal formulation showed a higher uptake than free p-rhASM/G-S in WT fibroblasts and a comparable uptake in NPD-B fibroblasts (Figs. 4 and 5). Moreover, the NPD-B fibroblasts exhibited a lower uptake of all loaded liposomes compared to WT fibroblasts, indicating an aberration in the uptake mechanism for liposomes (Fig. 4).

Macrophages are the main target cells in NPD-B. Thus, cellular uptake was investigated in the RAW 264.7 macrophage cell line. The loaded PS, PS-BMP and PG-BMP liposomal formulations showed higher cellular uptake by 2, 2.5 and 2.4 times relative to free p-rhASM/G-S, respectively, which indicates the preferable uptake of liposomes in RAW 264.7 cells (Figs. 4 and 6). The liposomal formulations with BMP lipid showed greater internalisation in RAW 264.7 cells, which indicates that the BMP lipid plays a role in the uptake mechanism. Since the uptake of the ASM enzyme via M-6-P receptors is impaired in ASM-deficient macrophages, liposomal formulations, following a different uptake pathway, showed higher levels of internalisation than free rhASM [16].

The colocalisation of p-rhASM/G-S in the lysosomes of RAW 264.7 cells was determined by calculating the Pearson's correlation coefficient (PCC) of LysoTracker Red and Alexa Fluor 488 from a total of 36 confocal pictures for each formulation. PCC quantifies the degree of colocalisation between the used fluorophores, in which 1 equals complete positive colocalisation, 0 equals random colocalisation, and −1 equals complete negative colocalisation [52]. The loaded liposomal formulations showed positive colocalisation between 0.34 and 0.47 compared to free p-rhASM/G-S, which had a random colocalisation (Fig. 7). These data suggest the improved lysosomal delivery of p-rhASM/G-S by the liposomal formulations, compared to free enzyme in RAW 264.7 cells.

From this study, the superior cellular internalisation of p-rhASM/G-S was observed with PS-BMP liposomes compared to other liposomal formulations in all tested cell models. Free p-rhASM/G-S and loaded PS-BMP liposomes have a similar cellular uptake in NPD-B fibroblasts; however, higher cellular uptake and lysosomal colocalisation in RAW 264.7 cells were observed with the loaded PS-BMP liposomes. Hence, this formulation was chosen for further investigation.

3.4. Cellular activity of ASM and reduction of accumulated lipids

To determine if the delivery of rhASM to the lysosomes of cells also leads to the reduction of sphingolipids, both ASM activity and a reduction in the amount of lyso-sphingomyelin, a deacylated form of sphingomyelin, were measured in WT and NPD-B fibroblasts. The residual ASM activity in tested NPD-B fibroblasts was 10%, relative to the ASM activity level in WT fibroblasts (Fig. 8). The primary accumulated material is sphingomyelin, but elevated levels of lyso-glycosphingolipids have been detected in the tissues and plasma of NPD-B patients [6,53]. As expected, the NPD-B fibroblasts showed a high

accumulation of lyso-sphingomyelin at 2525 pmol/g, compared to WT fibroblasts at 221 pmol/g (Fig. 9).

The incubation of NPD-B fibroblasts with free p-rhASM/G-S and the loaded PS-BMPliposomes led to restore the cellular ASM activity to 86% and 40%, respectively, relative to the WT fibroblasts. In comparison, non-treated NPD-B fibroblasts showed only 10% residual activity (Fig. 8). Therefore, we expected a reduction of the accumulated lipids when use the ASM-containing formulations. Indeed, significant reductions in the accumulated lyso-sphingomyelin (2525 pmol/g) in NPD-B fibroblasts were observed by free rhASM and loaded PS-BMP liposomes to 1138 and 729 pmol/g, respectively. Strikingly, non-loaded PS-BMP liposomes showed a reduction in lyso-sphingomyelin by 55% in NPD-B fibroblasts (Fig. 9). Although further investigation is needed, a possible explanation can be that the delivery of BMP lipid to lysosomes has contributed to the increased activity of residual ASM (Fig. 8), an effect that has been reported before [31,54,55]. Despite the unexpected reduction in lyso-sphingomyelin (55% reduction) induced by non-loaded liposomes, the biggest reduction of 71% was obtained with the loaded PS-BMP liposomal formulation, demonstrating the superiority of liposomal ASM formulation in substrate reduction.

3.5. Fluorometric sphingomyelin degradation assay

The off-target degradation of sphingomyelin by free rhASM could potentially lead to undesirable effects, as discussed earlier [10]. To test the level of protection provided by liposomes, extracellular sphingomyelin conversion by free p-rhASM/G-S was tested *in vitro* and compared to PS-BMP liposomal formulations. To allow direct interaction, the formulations (1 μg for formulations with enzyme) were incubated for four hours with different amounts of pure sphingomyelin. The amount of degraded sphingomyelin is directly proportional to the measured fluorescent units. At different concentrations of sphingomyelin (11, 33, 66, 100 μM), the conversion of sphingomyelin by loaded PS-BMP was lower by 65%, 65%, 61% and 53% relative to free p-rhASM/G-S. On average, the conversion was reduced by 61% (Fig. 10).

These results show that the liposomal formulation may have a superiority over free rhASM in preventing systemic degradation of sphingomyelin in the circulation. Furthermore, the amount of enzyme that is sequestered from the environment by liposomal confinement could be improved by increasing the molar ratio of BMP lipid in addition to removal of p-rhASM/G-S bound to the surface of liposomes using proteinase K.

4. Conclusions

RhASM was produced using HEK293T/17 and purified using a single-step purification to yield 4 mg/L. The purified rhASM was incorporated into four liposomal formulations with different compositions. PS-BMP liposomes showed the highest encapsulation efficiency and superior cellular uptake by WT fibroblasts, NPD-B fibroblasts, and RAW 264.7 cells compared to other liposomal formulations. The accumulated sphingomyelin in NPD-B fibroblasts was reduced by 71% and 55% using loaded PS-BMP liposomes and free enzyme, respectively. Importantly, the undesirable degradation of sphingomyelin by free enzyme was significantly reduced to 61% when using the loaded PS-BMP liposomes.

Incorporation of rhASM into PS-BMP liposomes has improved the efficacy and reduced the off-target degradation of sphingomyelin compared to free rhASM in the *in vitro* studies.

Acknowledgements

This work was funded by Saudi Food and Drug Authority (Riyadh, Saudi Arabia) via a PhD scholarship to Mohammed H. Aldosari. R.P. de Vries is funded by a VENI grant from the Netherlands Organization for Scientific Research. The funders had no role in study design, data collection and analysis, decision to publish, or preparation of the manuscript.

Human and animal rights

Informed consent was obtained for using of human tissues in the study in compliance with the Declaration of Helsinki [56].

Declaration of interest

None.

Appendix A. Supplementary material

Supplementary data to this article can be found online at https://doi.org/10.1016/j.ejpb.2019.02.019.

References

[1] E.H. Schuchman, R.J. Desnick, Types A and B Niemann-Pick disease, Mol. Genet. Metab. 120 (2017) 27–33.
[2] E.H. Schuchman, The pathogenesis and treatment of acid sphingomyelinase-deficient Niemann-Pick disease, J. Inherit. Metab. Dis. 30 (2007) 654–663.
[3] B. Otterbach, W. Stoffel, Acid sphingomyelinase-deficient mice mimic the neurovisceral form of human lysosomal storage disease (Niemann-Pick disease), Cell 81 (1995) 1053–1061.
[4] M.M. McGovern, R. Avetisyan, B.-J. Sanson, et al., Disease manifestations and burden of illness in patients with acid sphingomyelinase deficiency (ASMD), Orphanet J. Rare Dis. 12 (2017) 41.
[5] E. Jessop, S. Upadhyaya, Ultra orphan drugs: the NHS model for managing extremely rare diseases, Expert Opin. Orphan Drugs 2 (2014) 1301–1308.
[6] M.P. Wasserstein, G.A. Diaz, R.H. Lachmann, et al., Olipudase alfa for treatment of acid sphingomyelinase deficiency (ASMD): safety and efficacy in adults treated for 30 months, J. Inherit. Metab. Dis. (2018) 1–10.
[7] A Long-term study of olipudase alfa in patients with acid sphingomyelinase deficiency. ClinicalTrials.gov, < https://clinicaltrials.gov/ct2/show/NCT02004704 > (accessed 20 July 2018).
[8] Efficacy, safety, pharmacodynamic, and pharmacokinetics study of olipudase alfa in patients with acid sphingomyelinase deficiency. ClinicalTrials.gov, < https://clinicaltrials.gov/ct2/show/NCT02004691 > (accessed 20 July 2018).
[9] Safety, tolerability, PK, and efficacy evaluation of repeat ascending doses of olipudase Alfa in pediatric patients < 18 Years of age with acid sphingomyelinase deficiency. ClinicalTrials.gov, < https://clinicaltrials.gov/ct2/show/NCT02292654 > (accessed 20 July 2018).
[10] J.M. Murray, A.M. Thompson, A. Vitsky, et al., Nonclinical safety assessment of recombinant human acid sphingomyelinase (rhASM) for the treatment of acid sphingomyelinase deficiency: the utility of animal models of disease in the toxicological evaluation of potential therapeutics, Mol. Genet. Metab. 114 (2015) 217–225.
[11] R. Kolesnick, The therapeutic potential of modulating the ceramide/sphingomyelin pathway, J. Clin. Invest. 110 (2002) 3–8.
[12] S. Spiegel, A.H. Merrill, Sphingolipid metabolism and cell growth regulation, FASEB J. 10 (1996) 1388–1397.
[13] E. Gulbins, S.Walter, K.A. Becker, et al., A central role for the acid sphingomyelinase/ceramide system in neurogenesis and major depression. J. Neurochem. 134, 183–192.
[14] T. Levade, N. Augé, R.J. Veldman, et al., Sphingolipid mediators in cardiovascular cell biology and pathology, Circ. Res. 89 (2001) 957–968.
[15] K. Ferlinz, R. Hurwitz, G. Vielhaber, et al., Occurrence of two molecular forms of human acid sphingomyelinase, Biochem. J. 301 (1994) 855–862.
[16] R. Dhami, E.H. Schuchman, Mannose 6-phosphate receptor-mediated uptake is defective in acid sphingomyelinase-deficient macrophages: implications for Niemann-Pick disease enzyme replacement therapy, J. Biol. Chem. 279 (2004) 1526–1532.
[17] J. Rappaport, C. Garnacho, S. Muro, Clathrin-mediated endocytosis is impaired in type A-B Niemann-Pick disease model cells and can be restored by ICAM-1-mediated enzyme replacement, Mol. Pharm. 11 (2014) 2887–2895.
[18] J. Rappaport, R.L. Manthe, C. Garnacho, et al., Altered clathrin-independent endocytosis in type A Niemann-Pick disease cells and rescue by ICAM-1-targeted enzyme delivery, Mol. Pharm. 12 (2015) 1366–1376.
[19] K. Fu, D.W. Pack, A.M. Klibanov, et al., Visual evidence of acidic environment within degrading poly(lactic-co-glycolic acid) (PLGA) microspheres, Pharm. Res. 17 (2000) 100–106.
[20] M. van de Weert, W.E. Hennink, W. Jiskoot, Protein instability in poly(lactic-co-glycolic acid) microparticles, Pharm. Res. 17 (2000) 1159–1167.
[21] L. Sercombe, T. Veerati, F. Moheimani, et al., Advances and challenges of liposome assisted drug delivery, Front. Pharmacol. 6 (2015) 286.
[22] F. Ahsan, I.P. Rivas, M.A. Khan, et al., Targeting to macrophages: role of physicochemical properties of particulate carriers–liposomes and microspheres–on the

phagocytosis by macrophages, J. Control. Release 79 (2002) 29–40.
[23] R. Dhami, X. He, R.E. Gordon, et al., Analysis of the lung pathology and alveolar macrophage function in the acid sphingomyelinase deficient mouse model of Niemann-Pick disease, Lab. Invest. 81 (2001) 987–999.
[24] T. Daemen, M. Velinova, J. Regts, et al., Different intrahepatic distribution of phosphatidylglycerol and phosphatidylserine liposomes in the rat, Hepatology 26 (1997) 416–423.
[25] X. Yan, G.L. Scherphof, J.A.A.M. Kamps, Liposome opsonization, J. Liposome Res. 15 (2005) 109–139.
[26] S.C. Semple, A. Chonn, P.R. Cullis, Interactions of liposomes and lipid-based carrier systems with blood proteins: relation to clearance behaviour in vivo, Adv. Drug Deliv. Rev. 32 (1998) 3–17.
[27] D. Liu, F. Liu, Y.K. Song, Recognition and clearance of liposomes containing phosphatidylserine are mediated by serum opsonin, Biochim. Biophys. Acta 1235 (1995) 140–146.
[28] G. Scherphof, F. Roerdink, M. Waite, et al., Disintegration of phosphatidylcholine liposomes in plasma as a result of interaction with high-density lipoproteins, Biochim. Biophys. Acta 542 (1978) 296–307.
[29] H. Harashima, K. Sakata, K. Funato, et al., Enhanced hepatic uptake of liposomes through complement activation depending on the size of liposomes, Pharm. Res. 11 (1994) 402–406.
[30] P. Aggarwal, J.B. Hall, C.B. McLeland, et al., Nanoparticle interaction with plasma proteins as it relates to particle biodistribution, biocompatibility and therapeutic efficacy, Adv. Drug Deliv. Rev. 61 (2009) 428–437.
[31] T. Linke, G. Wilkening, S. Lansmann, et al., Stimulation of acid sphingomyelinase activity by lysosomal lipids and sphingolipid activator proteins, Biol. Chem. 382 (2001) 283–290.
[32] Z.-J. Xiong, J. Huang, G. Poda, et al., Structure of human acid sphingomyelinase reveals the role of the saposin domain in activating substrate hydrolysis, J. Mol. Biol. 428 (2016) 3026–3042.
[33] W. Möbius, E. van Donselaar, Y. Ohno-Iwashita, et al., Recycling compartments and the internal vesicles of multivesicular bodies harbor most of the cholesterol found in the endocytic pathway, Traffic 4 (2003) 222–231.
[34] V.O. Oninla, B. Breiden, J.O. Babalola, et al., Acid sphingomyelinase activity is regulated by membrane lipids and facilitates cholesterol transfer by NPC2, J. Lipid Res. 55 (2014) 2606–2619.
[35] R.W. Jenkins, D. Canals, Y.A. Hannun, Roles and regulation of secretory and lysosomal acid sphingomyelinase, Cell. Signal. 21 (2009) 836–846.
[36] R.P. de Vries, E. de Vries, B.J. Bosch, et al., The influenza A virus hemagglutinin glycosylation state affects receptor-binding specificity, Virology 403 (2010) 17–25.
[37] M. Moll, A. Kaufmann, A. Maisner, Influence of N-glycans on processing and biological activity of the nipah virus fusion protein, J. Virol. 78 (2004) 7274–7278.
[38] H.H. Freeze, C. Kranz, Endoglycosidase and glycoamidase release of N-linked glycans, Curr. Protoc. Mol. Biol. 0 (2010) 17, https://doi.org/10.1002/0471142727.mb1713as89 Epub ahead of print January.
[39] H. Zhang, Thin-film hydration followed by extrusion method for liposome preparation, Methods Mol. Biol. 1522 (2017) 17–22.
[40] S.G. Antimisiaris, Preparation of DRV liposomes, Methods Mol. Biol. 1522 (2017) 23–47.
[41] C.H. Fiske, Y. Subbarow, The colorimetric determination of phosphorus, J. Biol. Chem. 66 (1925) 375–400.
[42] E.G. Bligh, W.J. Dyer, A rapid method of total lipid extraction and purification, Can. J. Biochem. Physiol. 37 (1959) 911–917.
[43] M. Voorink-Moret, S.M.I. Goorden, A.B.P. van Kuilenburg, et al., Rapid screening for lipid storage disorders using biochemical markers, Mol. Genet. Metab. 123 (2018) 76–84.
[44] A. Hasilik, The early and late processing of lysosomal enzymes: proteolysis and compartmentation, Experientia 48 (1992) 130–151.
[45] K. von Figura, A. Hasilik, Lysosomal enzymes and their receptors, Annu. Rev. Biochem. 55 (1986) 167–193.
[46] S. Lansmann, K. Ferlinz, R. Hurwitz, et al., Purification of acid sphingomyelinase from human placenta: characterization and N-terminal sequence, FEBS Lett. 399 (1996) 227–231.
[47] H. Qiu, T. Edmunds, J. Baker-Malcolm, et al., Activation of human acid sphingomyelinase through modification or deletion of C-terminal cysteine, J. Biol. Chem. 278 (2003) 32744–32752.
[48] A.C. Dalton, W.A. Barton, Over-expression of secreted proteins from mammalian cell lines, Protein Sci. 23 (2014) 517–525.
[49] X. He, S.R. Miranda, X. Xiong, et al., Characterization of human acid sphingomyelinase purified from the media of overexpressing Chinese hamster ovary cells, Biochim. Biophys. Acta 1432 (1999) 251–264.
[50] J.H. Kang, W.Y. Jang, Y.T. Ko, The effect of surface charges on the cellular uptake of liposomes investigated by live cell imaging, Pharm. Res. 34 (2017) 704–717.
[51] J. Kamps, G. Scherphof, Receptor versus non-receptor mediated clearance of liposomes, Adv. Drug Deliv. Rev. 32 (1998) 81–97.
[52] J. Adler, I. Parmryd, Quantifying colocalization by correlation: the Pearson correlation coefficient is superior to the Mander's overlap coefficient, Cytometry A 77 (2010) 733–742.
[53] W.-L. Chuang, J. Pacheco, S. Cooper, et al., Lyso-sphingomyelin is elevated in dried blood spots of Niemann-Pick B patients, Mol. Genet. Metab. 111 (2014) 209–211.
[54] T. Kolter, K. Sandhoff, Principles of lysosomal membrane digestion: stimulation of sphingolipid degradation by sphingolipid activator proteins and anionic lysosomal lipids, Annu. Rev. Cell Dev. Biol. 21 (2005) 81–103.
[55] T. Kirkegaard, A.G. Roth, N.H.T. Petersen, et al., Hsp70 stabilizes lysosomes and reverts Niemann-Pick disease-associated lysosomal pathology, Nature 463 (2010) 549–553.
[56] World Medical Association, World Medical Association Declaration of Helsinki: ethical principles for medical research involving human subjects, JAMA 310 (2013) 2191–2194.